

Published in final edited form as:

*Nat Microbiol.* ; 2: 17100. doi:10.1038/nmicrobiol.2017.100.

## Nutrient recycling facilitates long-term stability of marine microbial phototroph-heterotroph interactions

Joseph A. Christie-Oleza<sup>1,\*</sup>, Despoina Sousoni<sup>1</sup>, Matthew Lloyd<sup>1</sup>, Jean Armengaud<sup>2</sup>, and David J. Scanlan<sup>1</sup>

<sup>1</sup>School of Life Sciences, University of Warwick, Coventry CV4 7AL, UK

<sup>2</sup>CEA, DRF/Joliot/DMTS/ SPI/Li2D, Laboratory "technological Innovations for Detection and Diagnostic", Bagnols-sur-Cèze, F-30207, France

### Abstract

Biological interactions underpin the functioning of marine ecosystems, be it via competition, predation, mutualism, or symbiosis processes. Microbial phototroph-heterotroph interactions propel the engine that results in the biogeochemical cycling of individual elements and are critical for understanding and modelling global ocean processes. Unfortunately, studies thus far have focused on exponentially-growing cultures in nutrient-rich media, meaning knowledge of such interactions under *in situ* conditions is rudimentary at best. Here, we performed long-term phototroph-heterotroph co-culture experiments under nutrient-amended and natural seawater conditions which showed that it is not the concentration of nutrients but rather their circulation that maintains a stable interaction and a dynamic system. Using the *Synechococcus-Roseobacter* interaction as a model phototroph-heterotroph case study we show that whilst *Synechococcus* is highly specialised for carrying out photosynthesis and carbon-fixation it relies on the heterotroph to re-mineralise the inevitably leaked organic matter making nutrients circulate in a mutualistic system. In this sense we challenge the general belief that marine phototrophs and heterotrophs compete for the same scarce nutrients and niche space, but instead suggest these organisms more likely benefit from each other because of their different levels of specialization and complementarity within long-term stable-state systems.

---

Users may view, print, copy, and download text and data-mine the content in such documents, for the purposes of academic research, subject always to the full Conditions of use:[http://www.nature.com/authors/editorial\\_policies/license.html#terms](http://www.nature.com/authors/editorial_policies/license.html#terms)

\*Corresponding author: School of Life Sciences, University of Warwick, Coventry CV4 7AL, UK, Tel.: +44 (0) 2476 572969. Fax: +44 (0) 2476 532701, j.christie-oleza@warwick.ac.uk.

#### Data availability statement

The data that support the findings of this study are available as Supplementary Information, Figures and Tables.

#### Author Contributions

J.A.C.-O. and D.J.S. conceived the study. J.A.C.-O. designed the experiments. J.A.C.-O., D.S., and M.L. performed the experiments. J.A. carried out the proteomic analyses. J.A.C.-O. analysed the data. J.A.C.-O. and D.J.S. wrote the paper with contributions from J.A.

#### Competing Financial Interests

The authors declare no conflict of interest.

## Introduction

Marine primary production is mainly driven by microscopic phytoplankton since phototrophic picocyanobacteria and picoeukaryotes contribute to almost all photosynthesis that takes place in the vast photic zones of the oligotrophic open ocean<sup>1</sup>. Picocyanobacteria (i.e. *Prochlorococcus* and *Synechococcus*) are the numerically most abundant primary producers on Earth<sup>2</sup> and their abundance is predicted to increase due to climate change<sup>3</sup>. Marine planktonic microorganisms generally show stable cell numbers, with growth and loss largely balanced<sup>4,5</sup>. Ultimately, all primary production will be converted into particulate or dissolved organic matter (DOM) which becomes the main source of carbon and energy for the complex marine food web<sup>6,7</sup>. DOM is thought to be generated by cell death, viral lysis and inefficient grazing, but also living organisms are known to be, *per se*, inevitably or ‘intentionally’ leaky, e.g. through the production of extracellular vesicles<sup>8</sup>, active efflux processes or, simply, permeable membrane leakage. In this sense, phytoplankton drive bacterial community dynamics as they are the main suppliers of organic matter<sup>9</sup>. Interestingly, despite reports showing how marine picocyanobacteria acquire simple organic compounds such as amino acids or glucose<sup>10,11</sup>, these organisms generally cannot utilise complex DOM as they lack the necessary pool of secreted enzymes<sup>12,13</sup>, potentially creating a dependence on remineralised nutrients released by the heterotrophic community.

Here, we set out to understand the long-standing anecdotal observation that cultures of phototrophic organisms are more robust and have a much longer lifespan when indigenous heterotrophic bacterial ‘contaminants’ are present, in both natural and nutrient amended seawater. In phototroph-heterotroph systems, heterotrophs clearly benefit through the acquisition of organic matter as a source of carbon and energy<sup>14</sup>. From the phototroph perspective, previous studies concluded that the interaction is based on the heterotrophic scavenging of oxidative stress<sup>15–18</sup>, supply of vitamins<sup>19–24</sup> or the exchange of growth factors<sup>25</sup>. These are clearly important physiological dependency events that have occurred in strong mutualistic interactions during the evolution of streamlined genomes in stable environments<sup>26</sup>. However, these may only be species-specific co-evolution events and do not explain the general aspects that underpin phototroph-heterotroph interactions. For example, unlike *Prochlorococcus*, which is deficient in catalase-peroxidase mechanisms involved in oxygen radical protection and detoxification<sup>17</sup>, and picoeukaryotes, which are usually deficient in vitamin production<sup>27</sup>, marine *Synechococcus* are capable of both these physiological functions, but still require heterotrophic microbes for long-lasting growth as shown in this study.

Whilst previous reports analysing marine picocyanobacteria-heterotroph interactions have focused on exponential phase cultures in nutrient-rich media<sup>18,28–31</sup>, we focus here for the first time on the long-term stable-state growth phase, both in rich media and natural oligotrophic seawater. We provide robust evidence to suggest that mutualistic phototroph-heterotroph interactions are based on nutrient cycling. The phototroph inherently produces and leaks organic matter in the form of photosynthate that allows growth of the heterotroph. In exchange, the heterotroph i) avoids the build-up of photosynthate which, for as-yet-unknown reasons, becomes toxic to the phototroph (in nutrient-rich medium), or ii)

‘unlocks’ inorganic nutrients within the photosynthate that can then be re-used by the phototroph to continue fixing CO<sub>2</sub> (in natural seawater).

## Results

### Physiology of long-term *Synechococcus*-heterotroph co-cultures

We assessed the growth of axenic *Synechococcus* sp. WH7803 in ASW medium with different *Roseobacter* strains as well as various heterotrophic bacterial ‘contaminant’ strains obtained from other non-axenic *Synechococcus* cultures (Figure 1a and 1b). In the presence of various heterotrophs, *Synechococcus* sp. WH7803 cultures could persist for over 10 months whereas axenic cultures died after 4-6 weeks. No significant difference in growth rate or maximum cell densities was observed for *Synechococcus* sp. WH7803 when grown in the presence/absence of the heterotroph during exponential phase (38.2 and 38.7 h doubling times, respectively) (Figure 1c). Some of the heterotrophs tested seemed less efficient in stably-sustaining *Synechococcus* in long-term culture but after an initial death phase of the phototroph, the co-culture re-established high cell density (i.e. Figure 1a, and *Tropicibacter* sp. in Figure 1c). *R. pomeroyi* DSS-3 also sustained growth of other axenic *Synechococcus* strains (i.e. WH8102 and WH7805) (Supplementary Figure 1 and Supplementary Note 1).

The heterotrophs in co-culture with *Synechococcus* reached high cell densities despite the absence of any exogenous addition of an organic source of carbon and energy, vitamins or nutrient requirements (Figure 1d and Supplementary Note 2). Hence, there is a clear benefit from this mutualistic interaction through the acquisition of photosynthate. This beneficial effect is unsurprisingly higher if *Synechococcus* is alive and continuously producing and releasing organic matter (Supplementary Figure 2).

### The death of axenic *Synechococcus* cultures in ASW medium is due to the accumulation of organic matter

The death of *Synechococcus* cultures was not due to the accumulation of reactive oxygen species, variation in pH or to the lack of auxotrophic supplements (e.g. vitamins) or nutrients (see Supplementary Note 3 and Supplementary Figure 3), but rather due to the accumulation of organic matter. The accumulation of carbohydrate and protein was monitored over time in axenic *Synechococcus* cultures showing up to 200 and 400 µg ml<sup>-1</sup> of carbohydrate and protein, respectively, being produced after 35 days (Supplementary Figure 4a). The large quantity of protein compared to carbohydrates indicates that *Synechococcus* produces N-rich DOM. This build-up of DOM (0.06% w/v when considering only protein and carbohydrates) is potentially toxic to *Synechococcus*. Indeed, via the addition of known concentrations of exogenous organic matter (i.e. peptone and yeast extract, Supplementary Figure 4b) we observed that concentrations of DOM between 0.01-0.1% w/v accelerated the death of axenic *Synechococcus* sp. WH7803 cultures, whereas the presence of *R. pomeroyi* DSS-3 rescued the culture except when the concentration of organic carbon was too high (1% w/v).

## Molecular interactions in ASW phototroph-heterotroph co-cultures assessed by proteomics

Comparative proteomics analysis (Supplementary Tables 1 and 2) suggests:

- i) *Synechococcus* is a specialised biological system for carrying out photosynthesis and CO<sub>2</sub> fixation. Almost 45% of *Synechococcus* sp. WH7803 protein abundance had a direct role in photosynthesis or CO<sub>2</sub> fixation (Table 1). This percentage increases when other directly linked processes to photosynthesis and CO<sub>2</sub> fixation are included (e.g. ATP synthase complex, oxidative phosphorylation or biosynthetic pathways of tetrapyrrole ring systems).
- ii) Comparative analysis of *Synechococcus* when grown in axenic culture versus in co-culture showed a small number of differentially expressed proteins (14 and 27 proteins respectively, increased or decreased when using stringent cut-off values: fold change >2 and p-value <0.01; Table 2). Interestingly, those proteins with the highest increase in co-culture were five proteins of unknown function. Curiously, the two most abundantly increased proteins, P1017 and P1706 (38.7 and 6.3 fold increase in co-culture, respectively), both contain the COG5361 with DUF1254 and DUF1214 conserved regions (Supplementary Figure 5a). The architecture of COG5361 is conserved and encoded in almost 20% of genomes through all domains of life (Supplementary Figure 5b and Supplementary Table 3). The fact most of the highest differentially expressed proteins are of unknown function mirrors observations in short-term phototroph-heterotroph co-culture experiments<sup>28,30,31</sup>, and highlights our current lack of knowledge of specific microbial interaction processes. We also detected an increase in proteins involved in pyruvate and oxaloacetate biosynthesis from phosphoenolpyruvate (i.e. pyruvate kinase and phosphoenolpyruvate carboxylase), favouring the citric acid cycle, when *R. pomeroyi* was present. Other proteins with an increased abundance in the presence of *R. pomeroyi* included those involved in twitching motility, amino acid transport, a glucose-methanol-choline like oxidoreductase, and a multi-copper oxidase amongst others (Table 2).
- iii) *Synechococcus* sp. WH7803 appears to utilise ammonium when grown in co-culture with *R. pomeroyi* despite ASW containing nitrate, a feature tentatively concluded from previous *Synechococcus-Vibrio* co-culture work<sup>28</sup>. This is suggested by the increase in proteins involved in ammonium assimilation via glutamate synthase and ammonium ligase, the shutdown of alternative pathways for acquiring nitrogen (e.g. nitrate or cyanate) and the reduction of proteins involved in the transamination/deamination of amino acids (Supplementary Table 2). This is highly suggestive of the heterotroph remineralising the organic matter produced by the phototroph and making ammonium available (see below).
- iv) At the functional level, a larger proportion of the *Synechococcus* proteome was allocated to the production of photosynthesis and membrane transport when the heterotroph was present (7 and 61%, respectively; Figure 2a). Such an obvious

increase in membrane transport protein capacity is largely due to the increase in abundance of two periplasmic binding proteins specific for amino acids and iron, both being highly detected proteins (0.5 and 0.9% of all *Synechococcus* proteins detected, respectively). Conversely, a decrease in mechanisms dealing with oxidative stress (12%, Figure 2a), vitamin/cofactor and nucleic acid metabolism was observed in co-culture (22 and 16%, respectively, Figure 2b). The 3.6-fold increase in abundance of a *Synechococcus* ABC-type amino acid transporter and the decrease in proteins related to central metabolic pathways (e.g. biosynthesis of nucleic acids and cofactors) in the presence of the heterotroph are potentially indicative of the hydrolysed organic matter becoming available and re-assimilated by the phototroph, as suggested previously during *Prochlorococcus-Alteromonas* interactions<sup>30</sup>.

- v) Only the 37 most abundant proteins of *R. pomeroyi* DSS-3 were detected as this organism represented only 6% of the cells within the co-culture at the time the samples were taken (Supplementary Table 2). Interestingly, ten of these proteins were components of active transport systems, mainly for amino acids or peptides, but also the sn-glycerol-3-phosphate ABC transporter (YP\_165509.1) was highly represented (over 2% NSAF). Altogether, active nutrient transport systems represented 20% of the total detected proteins without taking into account the major outer membrane porin (YP\_168626.1, 16.2% NSAF).

### Phototroph-heterotroph interactions in natural seawater

Given that nutrient availability is a key variable limiting ocean productivity and it is unlikely that organic matter will build-up to toxic levels in natural open ocean environments, we co-cultured *Synechococcus* and *R. pomeroyi* in filter-sterilised autoclaved natural seawater to assess phototroph-heterotroph interactions under natural (low nutrient) conditions. Despite reaching relatively low cell densities ( $\sim 10^5$  cells ml<sup>-1</sup>), the enhanced survival of *Synechococcus* was again only observed when the heterotroph was present (Figure 3a). Most interestingly, the phototroph reached a stable 1:10 cell density equilibrium with the heterotroph which was independent of the starting inoculum (Figure 3b), a density akin to that observed in natural surface seawater<sup>32</sup>. Increasing the nutrient load of the natural seawater (i.e. by adding ASW medium) showed culture cell yield was proportional to the concentration of nutrients present in the system, and only at high nutrient concentrations were cell yields limited by light (Supplementary Figure 3c).

### The phototroph-heterotroph mutualistic interaction is based on nutrient-exchange

Using nitrogen as a case study, we grew *Synechococcus* and *R. pomeroyi* in ASW with no N, as well as in ASW containing either 1mM nitrate or 0.01% (w/v) peptone ( $\cong 1$  mM N) as the only N source. As expected, monocultures of *Synechococcus* or *R. pomeroyi* could not utilise peptone or nitrate, respectively (Figure 3c and 3d) and behaved similarly to those cultures grown in ASW lacking N. Monocultures of *Synechococcus* and *R. pomeroyi* showed robust growth when grown with an accessible source of N (i.e. NO<sub>3</sub> or peptone, respectively) but initiated a cell density decline during stationary phase (Figure 3c and 3d). In contrast, when grown in co-culture, both strains reached similar cell yields but with cell

numbers being maintained across the 60 day timescale of the experiment. Most interestingly, each strain reached high growth yields even in those cultures in which the source of N was not accessible to them, highlighting a cross-feeding between the strains. Hence, regardless of the N source used in co-culture, even if inaccessible to one partner e.g. peptone for *Synechococcus* or nitrate for *R. pomeroyi*, an ultimate exchange of accessible N is achieved.

Further confirmation that the continuous supply of re-mineralised nutrients is the driving force of this mutualistic interaction was seen in the extended survival of *Synechococcus* in natural SW through periodic addition of small amounts of nutrients (1:1000 diluted ASW every 3-4 days, Figure 3e), mimicking the role of the heterotroph through a constant release of small amounts of nutrients.

We then determined which of the essential nutrients (i.e. N, P or trace metals) played a key role in the mutualistic interaction. Here, *Synechococcus* sp. WH7803 was again grown in axenic culture in natural SW, but this time small amounts of ASW (1:1000 diluted) lacking each one of the different nutrients were added (Figure 3f). All nutrients proved essential to sustain the survival of *Synechococcus* although cultures lacking a constant addition of P showed the strongest detrimental effect (i.e. similar to those where no nutrients were added, Figure 3f) despite the known phosphatase activity of *Synechococcus*33. This strongly suggests that the heterotroph plays an important role in the remineralisation of all essential nutrients for *Synechococcus* (i.e. N, P and metals).

### Nutrient analysis of SW cultures

Sterile SW was inoculated with *Synechococcus* sp. WH7803 alone, *R. pomeroyi* alone and a co-culture of both. Cultures were then incubated for 7 days under continuous light conditions to maintain phototrophic activity, followed by 7 days under continuous darkness. *Synechococcus* did not survive the dark period. DOC, DON, oxidised nitrogen (nitrate and nitrite) and ammonium was measured at the end of each period (Figure 4). DOC only showed a decrease in the presence of the heterotroph (from ~70 to 50  $\mu\text{M}$ ) whilst the concentration of DOC was maintained slightly higher in the presence of the phototroph (57  $\mu\text{M}$ ). Interestingly, *Synechococcus* depleted ammonium from the medium after the light incubation whilst *R. pomeroyi* was only able to regenerate it to its original level after the dark period (1.4  $\mu\text{M}$ ). Hence, the organic N contained within *Synechococcus* photosynthate is consumed by *R. pomeroyi* regenerating ammonium, which in turn is rapidly used by *Synechococcus*. *R. pomeroyi* cannot use or regenerate oxidised nitrogen and *Synechococcus* does not seem to deplete it completely from the medium. Phototroph monocultures enriched the DOM with DON (2.3  $\mu\text{M}$ ) decreasing the C:N ratio of marine DOM in seawater from 56 to 33 whereas the heterotroph increased the DOM's C:N ratio to 86-104 mainly due to the consumption of DON (Figure 4).

### Proteomic assessment of SW cultures

The proteome of *Synechococcus* sp. WH7803 incubated in seawater (Supplementary Table 4) showed a similar proteomic profile to that observed in nutrient-rich ASW medium (Table 1), with 43.5% of the cellular proteins dedicated to photosynthesis and CO<sub>2</sub> fixation. Membrane transport was the only protein category that showed a large variation, mainly due



to the detection of high amounts of potential P stress induced porins (i.e. YP\_001225958.1 and YP\_001225959.1, 5.3% and 1.0%, respectively) and a periplasmic binding protein component of an ABC transport system for phosphate (0.9%; Supplementary Table 5). Interestingly, while these phosphorus acquisition proteins increased >7-fold compared to their relative abundance in ASW medium, this was not the case for iron transport with ABC iron transporter levels very similar between the two conditions (0.68% in ASW and 0.54% in SW).

Comparative analysis of the *Synechococcus* proteome grown in axenic versus co-culture in natural seawater showed no major protein category differences (Figure 2). Indeed, only a small number of proteins were differentially detected in these conditions but, of these, a reduction in the abundance of enzymes involved in vitamin and cofactor biosynthesis was observed in the presence of the heterotroph (Supplementary Table 5).

As previously observed in ASW, *R. pomeroyi* devoted a large fraction of its proteome to active membrane transport (over 21%; mainly focussed on the uptake of amino acids and amine compounds) and an outer membrane porin (over 11%; Supplementary Table 5). Most interestingly, while *R. pomeroyi* DSS-3 devotes most of its membrane transporters to the uptake of organic compounds (59% versus 2.7% for inorganic compounds), *Synechococcus* sp. WH7803 shows a larger investment in acquiring inorganic compounds (85.2% versus 2.8% for organic compounds) highlighting how both organisms potentially target different substrates (Figure 5).

Finally, we carried out a comparative proteomics analysis of *R. pomeroyi* incubated in natural SW in the presence and absence of *Synechococcus* (Supplementary Table 6). Despite having a clear nutrient-starved pattern in both conditions, the heterotroph showed a remarkable switch from P starvation and a generalist-scavenging metabolism when alone, to N starvation and DON targeted metabolism in the presence of the phototroph (Supplementary Table 7 and Figure 5). When alone, *R. pomeroyi* showed an increased production of the PhoB regulon (24x), alkaline phosphatases (PhoD, 31x; PhoX, 2x), phosphate ABC transporter (3-7x) and phosphonate transport and metabolism (up to 57x). It also increased its metabolism involved in scavenging energy from a nutrient-poor environment, e.g. C1 metabolism (formate dehydrogenase, up to 337x; and carbon monoxide dehydrogenase, 3x), transporters for sulphonates (3x) and carbohydrates (2-83x), or benzoate catabolism (3-8x). On the other hand, *Synechococcus* seemed to be providing a constant source of amino acids and glycine betaine (increased detection of membrane transporters for these compounds, up to 16x), and vitamins as the anabolic pathways for thiamine and biotin were strongly decreased (up to 59x and 4x, respectively) (Supplementary Table 7).

## Discussion

Living organisms are never alone. The general belief that microbes compete for the same resources clashes with a basic concept in ecology whereby nutrients are recycled between phototrophic and heterotrophic organisms and, hence, how evolution favours specialisation and collaborative behaviour in co-existing populations<sup>26,34</sup>. Here, we demonstrate

experimentally how marine phototrophic and heterotrophic organisms represent key examples of this collaborative specialisation as highlighted by a clear functional partitioning of roles and the nutrient resources they target (Figure 5). Ultimately, this complementarity of functions implies that one group of organisms cannot survive without the other which favours a mutualistic interaction based on nutrient recycling. We believe this long-term mutualistic interaction is driven passively by the availability and balance of nutrients although further research is required in order to determine if the active production of specific signalling molecules are also involved, as was recently observed in marine diatom-bacterial interactions<sup>25</sup>.

Surprisingly, other than proteins involved in phosphate acquisition, *Synechococcus* appears to behave similarly in rich and poor media, dedicating a large fraction of its cellular resources to photosynthesis and CO<sub>2</sub> fixation (~50% of the proteome) under all culture conditions tested (Figure 5). Microorganisms with streamlined genomes are known to possess minimal gene regulation capacity and marine picocyanobacteria are similar in this respect<sup>2</sup>. Hence, it is perhaps unsurprising to observe only small differences in their proteome under varying culture conditions<sup>35</sup>. Previous transcriptomic studies analysing picocyanobacteria-heterotroph interactions also report relatively low fold changes in differentially-expressed genes between axenic and co-culture conditions<sup>28–31</sup>. Overall, the proteome analysis does suggest that the presence of *R. pomeroyi* allows *Synechococcus* to allocate more resources to carbon and energy pathways as the heterotroph may help perform other functions required for growth.

*Synechococcus* generates a considerable amount of complex photosynthate. It is unknown what fraction of this organic matter is intentionally excreted (i.e. through outer membrane vesicles<sup>8</sup> or protein secretion<sup>12</sup>) or arises as a consequence of leakage or cell lysis<sup>36</sup>. Whichever is the case, these streamlined phototrophs do not encode, or produce, a large array of active membrane transporters for organic compounds nor hydrolytic enzymes for the degradation of large polymeric organic matter<sup>12</sup> and seem to rely on the enzymatic activities of the heterotroph, a feature concordant with previous exoproteome data from *R. pomeroyi* where a large number of membrane transporters and poorly-characterised hydrolytic exoenzymes were detected in the presence of *Synechococcus*<sup>13</sup>. *R. pomeroyi* is a highly versatile generalist organism capable of using a wide range of substrates<sup>37–39</sup> and is alone able to degrade almost all labile organic matter produced by marine phytoplankton, a facet previously suggested for this organism<sup>13</sup> as well as another marine generalist *Alteromonas*<sup>40</sup>. Interestingly, *R. pomeroyi* showed a strong transition from an energy and phosphate scavenging metabolism when alone, to the preferential use of the organic forms within the photosynthate in the presence of *Synechococcus* i.e. amines and vitamins.

Our nutrient analyses and the proteomic response of *R. pomeroyi* to the presence of the phototroph suggest that *Synechococcus* produces N- (e.g. protein) and, probably, P-rich (e.g. glycerol-3-phosphate) DOM. The remineralisation of N from DOM or N-rich compounds by heterotrophs was previously reported<sup>41,42</sup>. The marine heterotrophic community will use DOM as a source of carbon and energy and, hence, the fraction used for the latter (i.e. respiration) will generate an excess of nutrients such as N or P. All primary-produced DOM in our long-term stable-state co-cultures or in balanced natural non-blooming euphotic



marine ecosystems, where biomass is generally maintained constant<sup>4,5</sup>, will ultimately be respired and, therefore, all nutrients re-mineralised. A small fraction of non-degraded DOM may become highly recalcitrant as part of the biological pump<sup>43</sup>, but this recalcitrant DOM is usually poor in N and P and contains extremely high C:N and C:P ratios<sup>44</sup>, highlighting the preference of heterotrophs for N- and P-rich DOM and the mineralisation of these macro-nutrients. Here, we prove that the recycling of all essential nutrients (i.e. N and metals, and especially P) is essential for maintaining the viability of *Synechococcus* suggesting this organism cannot ‘unlock’ these nutrients from its own photosynthate and requires the presence, in this case, of a generalist heterotroph or, in nature, of the succession of a specialised microbial community<sup>45</sup>. Picocyanobacteria seem to have evolved into ‘photosynthetic factories’, unable to sustain the burden of its large photosynthetic machinery during extended periods without a constant supply of inorganic nutrients and light.

Nutrient circulation is needed for a functional system (Figure 5). Inorganic macro- and micro-nutrients are constantly being made available in marine environments despite their rapid assimilation and incorporation into organic matter by microbes via the recycling of nutrients within the microbial loop. This connects phytoplankton and heterotrophic bacterial niche space since the former is limited by inorganic nutrients (e.g. N, P and iron) whereas the latter is normally carbon and energy limited. Based on these ‘niche’ requirements, both groups of organisms reach a stable balance in marine systems where relatively constant cell numbers are maintained<sup>5</sup>. Interestingly, our natural seawater work shows that the simple two-strain system we present here is a good surrogate of the general heterotroph-phototroph cell ratio in the oceans<sup>32</sup> (10:1) where cell yields are also limited by overall nutrient availability. Nevertheless, this *Synechococcus-R. pomeroyi* system lacks the presence of viruses or grazers which clearly play an important role in keeping the ecosystem ‘young’ and dynamic (see<sup>46</sup>) by speeding up the recirculation of nutrients. In any case, data we present here clearly demonstrate for the first time that the foundations of long-term self-sustained heterotroph-phototroph mutualistic interactions are based on nutrient recycling, which we posit is a basic concept in ecology.

## Materials and Methods

### Bacterial growth and culture conditions

Axenic marine *Synechococcus* strains WH7803, WH8102 and WH7805, and non-axenic strains CC9311 and BL107, were routinely grown in 100 ml ASW medium<sup>47</sup> contained in 250 ml Erlenmeyer flasks and incubated at 22°C at a light intensity of 10  $\mu\text{mol photons m}^{-2} \text{s}^{-1}$  with shaking (140 rpm). ASW contained no vitamin supplements, and with nitrogen (N) and phosphorus (P) supplied as 8.8 mM nitrate and 0.18 mM phosphate, unless indicated differently in the text. Natural seawater (SW) experiments were performed with water collected from the Gulf Stream in the Gulf of Mexico, supplied by Sigma (see Figure 4 for the Dissolved Organic Carbon (DOC) and Nitrogen measurements from this SW), autoclaved to inactivate viruses. The heterotrophic bacterium *Ruegeria pomeroyi* DSS-3 was used as the case study whilst other heterotrophs were *Roseobacter* strains: *Ruegeria lacuscaerulensis* ITI1157, *Dinoroseobacter shibae* DFL12 and *Roseobacter denitrificans* OCh114; isolates from *Synechococcus* sp. CC9311: *Tropicibacter* sp. and *Stappia* sp.; and

isolates from *Synechococcus* sp. BL107; *Paracoccus* sp., *Marinobacter* sp. and *Muricauda* sp. which were used to assess the generic nature of the specific observations. Isolates were identified by sequencing the near full-length 16S rRNA gene using the universal primers F27 and R149248. All heterotrophs were initially grown in marine broth (Difco). Cells were washed twice with autoclaved SW to eliminate nutrients before inoculating co-cultures. *Synechococcus* cell abundance was monitored by flow cytometry (BD FACScan) whilst viable heterotrophs were counted by colony forming units (CFU) on marine agar (Difco). A detailed comparison between CFU and flow cytometry cell counts can be found in the Supplementary Note 4 and Supplementary Figure 6. All experiments in this study were performed with independent biological triplicates.

### Preparation of cellular proteomes for nanoLC-MS/MS and data analysis

Shotgun proteomic analysis of cellular extracts of *Synechococcus* sp. WH7803 grown in ASW and SW medium in the presence and absence of *R. pomeroyi* DSS-3 was carried out to elucidate the molecular mechanisms occurring during the interaction process. We also analysed the proteome of *R. pomeroyi* DSS-3 in the presence and absence of the phototroph in SW conditions. Cell pellets were collected by centrifugation (3,000 g for 15 min at 4°C) using 10 and 400 ml of ASW and SW cultures, respectively. At the time point of collection (35 days for ASW and 10 days for SW), the heterotroph represented 6% and 69% of the cells within the co-culture in ASW and SW, respectively. Considering *Synechococcus* sp. WH7803 and *R. pomeroyi* DSS-3 cells are similar in size ( $1.0 \pm 0.2$  and  $1.1 \pm 0.1$   $\mu\text{m}$  in size, respectively, based on TEM measurements) we would expect these percentages to equate to the proportion of live biomass of each organism in the co-culture samples. Cell pellets were resuspended in 100  $\mu\text{l}$  NuPAGE LDS sample buffer 1X (Invitrogen) from which 30  $\mu\text{l}$  sample was analysed by SDS-PAGE as previously described<sup>49</sup>. ASW grown cell proteomes were resolved by SDS-PAGE in order to obtain six gel bands per sample that were individually analysed by nanoLC-MS/MS using a LTQ-Orbitrap XL hybrid mass spectrometer (ThermoFisher) coupled to an UltiMate 3000 LC system (Dionex-LC Packings) using conditions previously described<sup>50</sup>. SW grown cell proteomes were resolved by SDS-PAGE and a single gel band analysed using an Orbitrap Fusion mass spectrometer and the parameters previously described<sup>13</sup>. Compiled MS/MS spectra were searched against the annotated coding domain sequences (CDS) of *Synechococcus* sp. WH7803 and the updated annotation of *R. pomeroyi* DSS-351. Searches were carried out with Mascot software (Matrix Science, version 2.4.1) and protein identifications were validated using Scaffold (version 4.3.4, Proteome Software Inc.) in all cases using the standard parameters previously described<sup>13</sup>. Proteins were only validated with 2 or more different peptides. Protein quantification of ASW samples was performed by normalised spectral count abundance factor (NSAF)<sup>52</sup> whereas for the SW samples Progenesis Q1 was used (version 2.0.5, Nonlinear Dynamics, Waters). Protein categories were based on KEGG annotations with manual curation assessed by the Conserved Domain search tool from NCBI.

### Oxidative stress and nutrient analyses

Amplex Red Hydrogen Peroxide/Peroxidase Assay Kit (ThermoFisher) was used to measure oxidative stress in the cultures. Protein and carbohydrate analyses were performed with supernatants obtained from *Synechococcus* cultures grown in ASW. Cells were centrifuged

(13,000 g for 1 min) and supernatants were further filtered through a 0.2 µm diameter pore filter (Sartorius Minisart). Protein quantification was performed with the QuantiPro BCA assay kit (Sigma-Aldrich). Carbohydrate quantification was done using a phenol sulphuric acid assay<sup>53</sup>. Nutrient analyses were performed with SW supernatants obtained from *Synechococcus* and *R. pomeroyi* incubated individually and in co-culture after 7 days in optimal light conditions and, subsequently, from the same cultures after a 7-day incubation in the dark. DOC and Total Nitrogen (TN) measurements were performed using a TOC-L CPH Nutrient Analyser with the TNM-L accessory module (Shimadzu). NH<sub>3</sub> was measured using the FluoroSELECT Ammonia kit (Sigma-Aldrich) with a small modification to the manufacturer's recommendations in order to increase sensitivity (i.e. using 100 µl of sample per reaction). Nitrate and nitrite were measured with a fluorometric assay kit (Cayman Chemical, UK). Inorganic nitrogen (IN) was calculated by adding the NH<sub>3</sub> and oxidised nitrogen (NO<sub>3</sub> and NO<sub>2</sub>) measurements whilst Dissolved Organic Nitrogen (DON) was calculated by subtracting the inorganic nitrogen (IN) from the TN measurements (DON = TN – IN).

## Supplementary Material

Refer to Web version on PubMed Central for supplementary material.

## Acknowledgements

This work was supported by a NERC Independent Research Fellowship NE/K009044/1, UK Synthetic Biology Research Centre grant from EPSRC and BBSRC (BB/M017982/1) and the Commissariat à l'Energie Atomique et aux Energies Alternatives. DS was supported by a Central England NERC Training Alliance PhD scholarship via grant NE/L002493/1. We also acknowledge the technical support from the WPH Proteomic Facility at the University of Warwick.

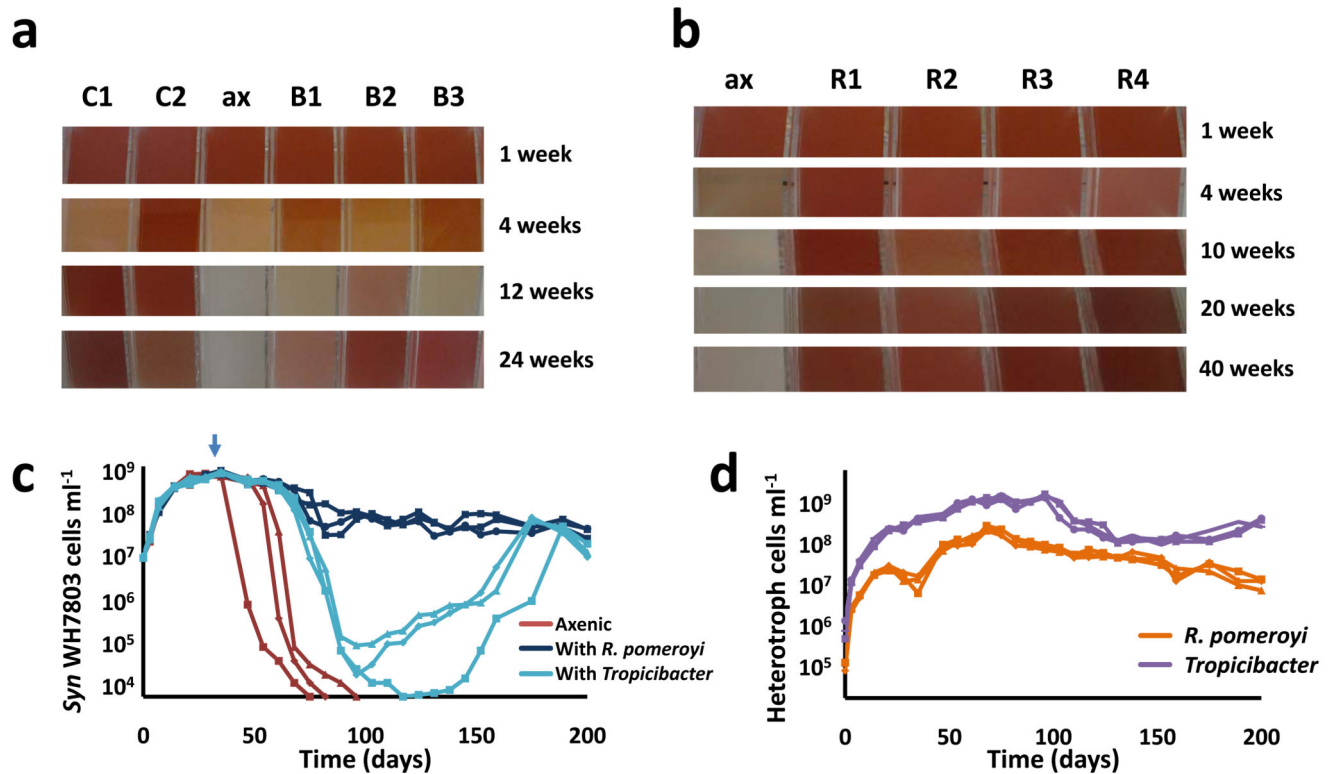
## References

1. Jardillier L, Zubkov MV, Pearman J, Scanlan DJ. Significant CO<sub>2</sub> fixation by small prymnesiophytes in the subtropical and tropical northeast Atlantic Ocean. *ISME J.* 2010; 4:1180–1192. [PubMed: 20393575]
2. Scanlan DJ, et al. Ecological genomics of marine picocyanobacteria. *Microbiol Mol Biol Rev.* 2009; 73:249–299. [PubMed: 19487728]
3. Flombaum P, et al. Present and future global distributions of the marine Cyanobacteria *Prochlorococcus* and *Synechococcus*. *Proc Natl Acad Sci USA.* 2013; 110:9824–9829. [PubMed: 23703908]
4. Jacquet S, Prieur L, Avois-Jacquet C, Lennon J-F, Vault D Short-timescale variability of picophytoplankton abundance and cellular parameters in surface waters of the Alboran Sea (western Mediterranean). *J Plankton Res.* 2002; 24:635–651.
5. Ribalet F, et al. Light-driven synchrony of *Prochlorococcus* growth and mortality in the subtropical Pacific gyre. *Proc Natl Acad Sci USA.* 2015; 112:8008–8012. [PubMed: 26080407]
6. McCarren J, et al. Microbial community transcriptomes reveal microbes and metabolic pathways associated with dissolved organic matter turnover in the sea. *Proc Natl Acad Sci USA.* 2010; 107:16420–16427. [PubMed: 20807744]
7. Sharma AK, et al. Distinct dissolved organic matter sources induce rapid transcriptional responses in coexisting populations of *Prochlorococcus*, *Pelagibacter* and the OM60 clade. *Environ Microbiol.* 2014; 16:2815–2830. [PubMed: 24118765]
8. Biller SJ, et al. Bacterial vesicles in marine ecosystems. *Science.* 2014; 343:183–186. [PubMed: 24408433]

9. Paver SF, et al. Interactions between specific phytoplankton and bacteria affect lake bacterial community succession. *Environ Microbiol.* 2013; 15:2489–2504. [PubMed: 23663352]
10. Munoz-Marin MC, et al. *Prochlorococcus* can use the Pro1404 transporter to take up glucose at nanomolar concentrations in the Atlantic Ocean. *Proc Natl Acad Sci USA.* 2013; 110:8597–8602. [PubMed: 23569224]
11. Yelton AP, et al. Global genetic capacity for mixotrophy in marine picocyanobacteria. *ISME J.* 2016; 10:2946–2957. [PubMed: 27137127]
12. Christie-Oleza JA, Armengaud J, Guerin P, Scanlan DJ. Functional distinctness in the exoproteomes of marine *Synechococcus*. *Environ Microbiol.* 2015; 17:3781–3794. [PubMed: 25727668]
13. Christie-Oleza JA, Scanlan DJ, Armengaud J. "You produce while I clean up", a strategy revealed by exoproteomics during *Synechococcus-Roseobacter* interactions. *Proteomics.* 2015; 15:3454–3462. [PubMed: 25728650]
14. Geng H, Belas R. Molecular mechanisms underlying *Roseobacter*-phytoplankton symbioses. *Curr Opin Biotechnol.* 2010; 21:332–338. [PubMed: 20399092]
15. Hunken M, Harder J, Kirst GO. Epiphytic bacteria on the Antarctic ice diatom *Amphiprora kufferathii* Manguin cleave hydrogen peroxide produced during algal photosynthesis. *Plant Biol.* 2008; 10:519–526. [PubMed: 18557912]
16. Morris JJ, Kirkegaard R, Szul MJ, Johnson ZI, Zinser ER. Facilitation of robust growth of *Prochlorococcus* colonies and dilute liquid cultures by "helper" heterotrophic bacteria. *Appl Environ Microbiol.* 2008; 74:4530–4534. [PubMed: 18502916]
17. Morris JJ, Johnson ZI, Szul MJ, Keller M, Zinser ER. Dependence of the cyanobacterium *Prochlorococcus* on hydrogen peroxide scavenging microbes for growth at the ocean's surface. *PLoS One.* 2011; 6:e16805. [PubMed: 21304826]
18. Sher D, Thompson JW, Kashtan N, Croal L, Chisholm SW. Response of *Prochlorococcus* ecotypes to co-culture with diverse marine bacteria. *ISME J.* 2011; 5:1125–1132. [PubMed: 21326334]
19. Amin SA, Parker MS, Armbrust EV. Interactions between diatoms and bacteria. *Microbiol Mol Biol Rev.* 2012; 76:667–684. [PubMed: 22933565]
20. Croft MT, Lawrence AD, Raux-Deery E, Warren MJ, Smith AG. Algae acquire vitamin B<sub>12</sub> through a symbiotic relationship with bacteria. *Nature.* 2005; 438:90–93. [PubMed: 16267554]
21. Sanudo-Wilhelmy SA, et al. Multiple B-vitamin depletion in large areas of the coastal ocean. *Proc Natl Acad Sci USA.* 2012; 109:14041–14045. [PubMed: 22826241]
22. Grant MA, Kazamia E, Cicuta P, Smith AG. Direct exchange of vitamin B<sub>12</sub> is demonstrated by modelling the growth dynamics of algal-bacterial co-cultures. *ISME J.* 2014; 8:1418–1427. [PubMed: 24522262]
23. Kazamia E, et al. Mutualistic interactions between vitamin B<sub>12</sub>-dependent algae and heterotrophic bacteria exhibit regulation. *Environ Microbiol.* 2012; 14:1466–1476. [PubMed: 22463064]
24. Durham BP, et al. Cryptic carbon and sulfur cycling between surface ocean plankton. *Proc Natl Acad Sci USA.* 2015; 112:453–457. [PubMed: 25548163]
25. Amin SA, et al. Interaction and signalling between a cosmopolitan phytoplankton and associated bacteria. *Nature.* 2015; 522:98–101. [PubMed: 26017307]
26. Morris JJ, Lenski RE, Zinser ER. The Black Queen Hypothesis: evolution of dependencies through adaptive gene loss. *mBio.* 2012; 3:e00036–12. [PubMed: 22448042]
27. Helliwell KE, et al. Cyanobacteria and eukaryotic algae use different chemical variants of vitamin B<sub>12</sub>. *Curr Biol.* 2016; 26:999–1008. [PubMed: 27040778]
28. Tai V, Paulsen IT, Phillippy K, Johnson DA, Palenik B. Whole-genome microarray analyses of *Synechococcus-Vibrio* interactions. *Environ Microbiol.* 2009; 11:2698–2709. [PubMed: 19659554]
29. Beliaev AS, et al. Inference of interactions in cyanobacterial-heterotrophic co-cultures via transcriptome sequencing. *ISME J.* 2014; 8:2243–2255. [PubMed: 24781900]
30. Aharonovich D, Sher D. Transcriptional response of *Prochlorococcus* to co-culture with a marine *Alteromonas*: differences between strains and the involvement of putative infochemicals. *ISME J.* 2016; 10:2892–2906. [PubMed: 27128996]

31. Biller SJ, Coe A, Chisholm SW. Torn apart and reunited: impact of a heterotroph on the transcriptome of *Prochlorococcus*. *ISME J.* 2016; 10:2831–2843. [PubMed: 27258949]
32. Parsons RJ, Breitbart M, Lomas MW, Carlson CA. Ocean time-series reveals recurring seasonal patterns of virioplankton dynamics in the northwestern Sargasso Sea. *ISME J.* 2012; 6:273–284. [PubMed: 21833038]
33. Mazard S, Wilson WH, Scanlan DJ. Dissecting the physiological response to phosphorus stress in marine *Synechococcus* isolates (*Cyanophyceae*). *J Phycol.* 2012; 48:94–105. [PubMed: 27009654]
34. Mas A, Jamshidi S, Lagadeuc Y, Eveillard D, Vandenkoornhuysse P. Beyond the Black Queen hypothesis. *ISME J.* 2016; 10:2085–2091. [PubMed: 26953598]
35. Sowell SM, et al. Proteomic analysis of stationary phase in the marine bacterium "Candidatus *Pelagibacter ubique*". *Appl Environ Microbiol.* 2008; 74:4091–4100. [PubMed: 18469119]
36. Grossowicz M, et al. *Prochlorococcus* in the lab and in silico: the importance of representing exudation. *Limnol Oceanogr.* 2017; 62:818–835.
37. Moran MA, et al. Genome sequence of *Silicibacter pomeroyi* reveals adaptations to the marine environment. *Nature.* 2004; 432:910–913. [PubMed: 15602564]
38. Newton RJ, et al. Genome characteristics of a generalist marine bacterial lineage. *ISME J.* 2010; 4:784–798. [PubMed: 20072162]
39. Christie-Oleza JA, Fernandez B, Nogales B, Bosch R, Armengaud J. Proteomic insights into the lifestyle of an environmentally relevant marine bacterium. *ISME J.* 2012; 6:124–135. [PubMed: 21776030]
40. Pedler BE, Aluwihare LI, Azam F. Single bacterial strain capable of significant contribution to carbon cycling in the surface ocean. *Proc Natl Acad Sci USA.* 2014; 111:7202–7207. [PubMed: 24733921]
41. Arandia-Gorostidi N, Weber PK, Alonso-Saez L, Moran XA, Mayali X. Elevated temperature increases carbon and nitrogen fluxes between phytoplankton and heterotrophic bacteria through physical attachment. *ISME J.* 2017; 11:641–650. [PubMed: 27922602]
42. Lidbury ID, Murrell JC, Chen Y. Trimethylamine and trimethylamine N-oxide are supplementary energy sources for a marine heterotrophic bacterium: implications for marine carbon and nitrogen cycling. *ISME J.* 2015; 9:760–769. [PubMed: 25148480]
43. Loh AN, Bauer JE, Druffel ER. Variable ageing and storage of dissolved organic components in the open ocean. *Nature.* 2004; 430:877–881. [PubMed: 15318218]
44. Jiao N, et al. Microbial production of recalcitrant dissolved organic matter: long-term carbon storage in the global ocean. *Nat Rev Microbiol.* 2010; 8:593–599. [PubMed: 20601964]
45. Teeling H, et al. Substrate-controlled succession of marine bacterioplankton populations induced by a phytoplankton bloom. *Science.* 2012; 336:608–611. [PubMed: 22556258]
46. Weinbauer MG, et al. *Synechococcus* growth in the ocean may depend on the lysis of heterotrophic bacteria. *J Plankton Res.* 2011; 33:1465–1476.
47. Wilson WH, Carr NG, Mann NH. The effect of phosphate status on the kinetics of cyanophage infection in the oceanic cyanobacterium *Synechococcus* sp WH7803. *J Phycol.* 1996; 32:506–516.
48. Lane, D. Nucleic acid techniques in bacterial systematics. Stackebrandt, EG., Goodfellow, M., editors. John Wiley; 1991. p. 115-175.
49. Hartmann EM, Allain F, Gaillard JC, Pible O, Armengaud J. Taking the shortcut for high-throughput shotgun proteomic analysis of bacteria. *Methods Mol Biol.* 2014; 1197:275–285. [PubMed: 25172287]
50. de Groot A, et al. Alliance of proteomics and genomics to unravel the specificities of Sahara bacterium *Deinococcus deserti*. *PLoS Genet.* 2009; 5:e1000434. [PubMed: 19370165]
51. Rivers AR, Smith CB, Moran MA. An updated genome annotation for the model marine bacterium *Ruegeria pomeroyi* DSS-3. *Stand Genomic Sci.* 2014; 9:11. [PubMed: 25780504]
52. Liu H, Sadygov RG, Yates JR 3rd. A model for random sampling and estimation of relative protein abundance in shotgun proteomics. *Anal Chem.* 2004; 76:4193–4201. [PubMed: 15253663]
53. Masuko T, et al. Carbohydrate analysis by a phenol-sulfuric acid method in microplate format. *Anal Biochem.* 2005; 339:69–72. [PubMed: 15766712]

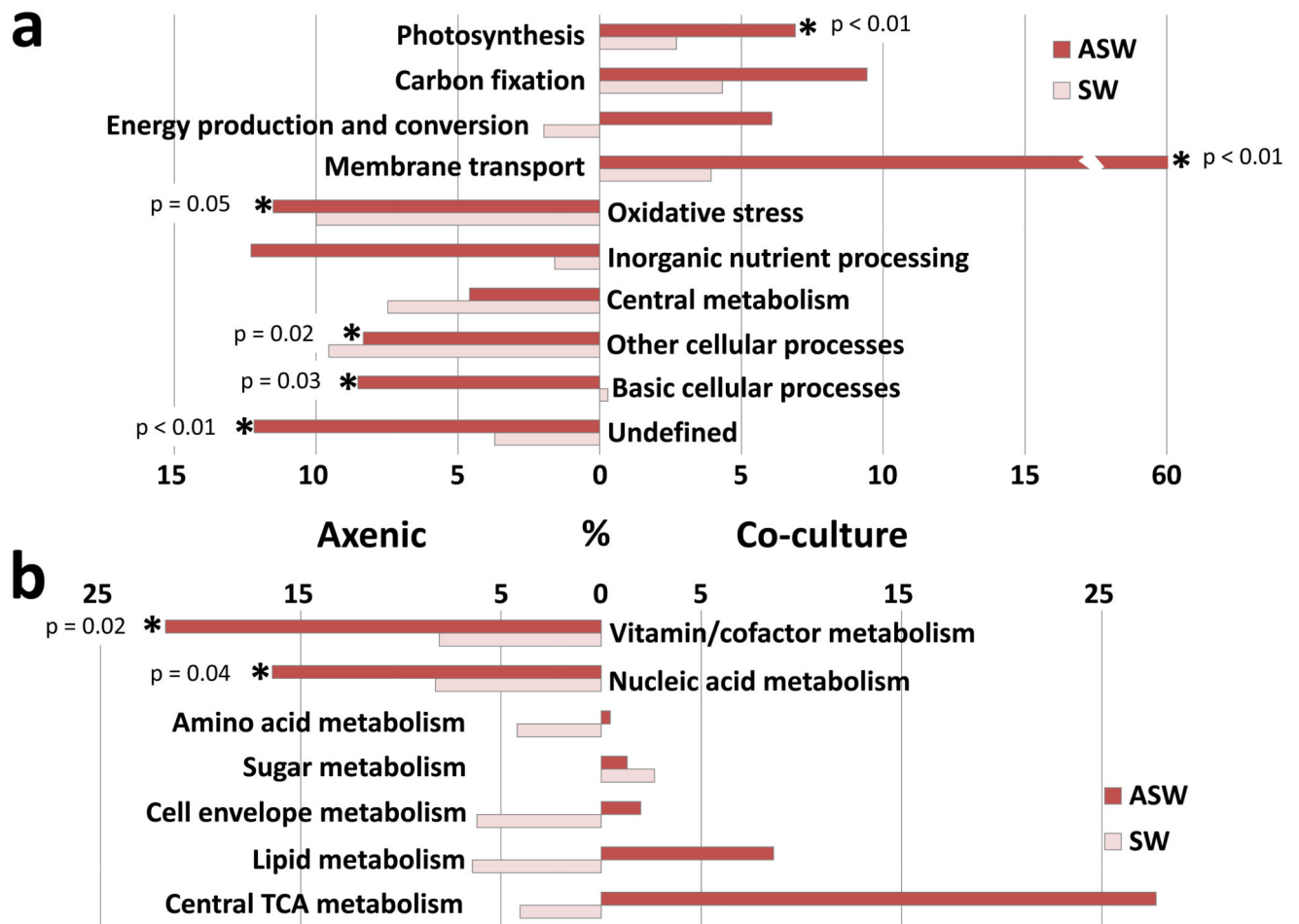




**Figure 1.**

*Synechococcus* sp. WH7803 grown in axenic (ax) culture and in co-culture with different heterotrophs. (a) *Synechococcus* sp. WH7803 grown for 24 weeks with heterotrophs isolated from other non-axenic *Synechococcus* strains and identified by partial 16S rDNA sequencing. C1 (*Tropicibacter* sp.) and C2 (*Stappia* sp.) were isolated from *Synechococcus* sp. CC9311 and B1 (*Paracoccus* sp.), B2 (*Marinobacter* sp.) and B3 (*Muricauda* sp.) were isolated from *Synechococcus* sp. BL107. (b) *Synechococcus* sp. WH7803 grown for 40 weeks with different *Roseobacter* strains: R1 (*R. pomeroyi* DSS-3), R2 (*Ruegeria lacuscaerulensis* ITI1157), R3 (*Dinoroseobacter shibae* DFL12) and R4 (*Roseobacter denitrificans* OCh114). The highly pigmented cultures observed in week 1 are typical of a healthy culture whereas white (bleached) cultures indicate dead *Synechococcus*. A representative culture of three biological replicates is shown in panels A and B. (c) Growth curves of *Synechococcus* sp. WH7803 in ASW in axenic culture and in the presence of the heterotrophs *R. pomeroyi* DSS-3 or *Tropicibacter* sp. The arrow indicates the time point at which cell were harvest for the proteomic analysis (35 days). (d) Growth curves of the heterotrophs *R. pomeroyi* DSS-3 and *Tropicibacter* sp. in the presence of *Synechococcus* sp. WH7803. *Synechococcus* cell counts were determined by flow cytometry and heterotrophic growth was monitored by colony forming units on Marine Agar plates. Three culture replicates (n=3) of each condition are represented in panels c and d.



**Figure 2.**

Comparative proteomic analysis of *Synechococcus* sp. WH7803 proteins detected in the absence (axenic) and presence of *R. pomeroyi* DSS-3 (co-culture) (n=3). (a) All categories and (b) subcategories from central metabolism are shown. Asterisks represent significant differences (*t*-test;  $p < 0.05$ ). Bars on the left indicate % increase in functional groups in axenic culture. Bars on the right indicate % increase in functional groups in co-culture.

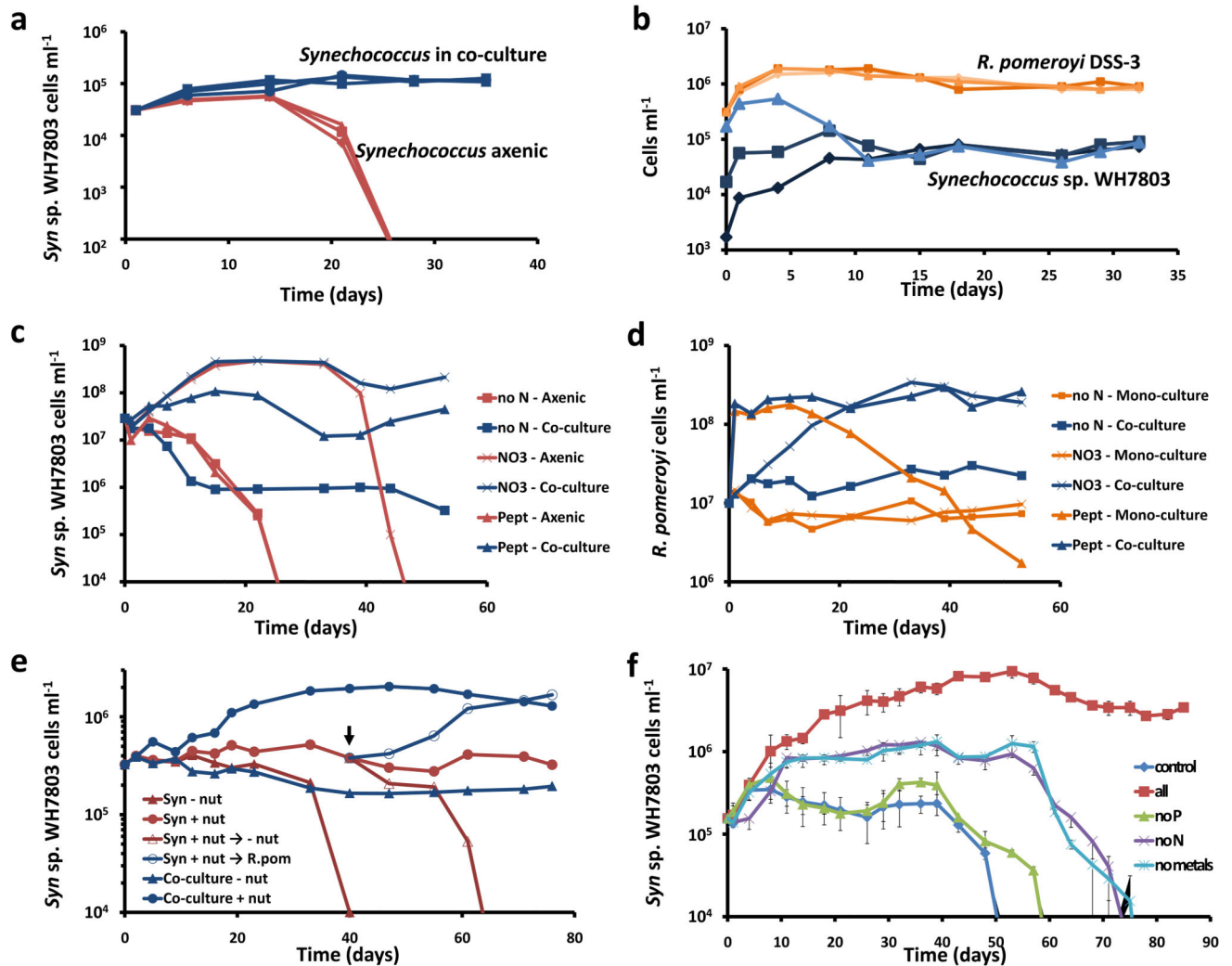


**Figure 3.**

Growth curves under nutrient limiting conditions. (a) Growth of *Synechococcus* sp. WH7803 in SW in the presence or absence of *R. pomeroyi* DSS-3. (b) Growth curves of *Synechococcus* sp. WH7803-*R. pomeroyi* DSS-3 co-cultures in SW where *Synechococcus* was inoculated at three different concentrations (i.e.  $\sim 10^3$ ,  $10^4$  and  $10^5$  cells  $\text{ml}^{-1}$ ). Three culture replicates ( $n=3$ ) of each condition are represented in panels A and B. Growth curves of (c) *Synechococcus* sp. WH7803 and (d) *R. pomeroyi* DSS-3 grown in axenic culture and in co-culture in ASW with no N and nitrate and peptone as the only source of N. (e) Growth curves of *Synechococcus* sp. WH7803 in SW with (+ nut) and without (- nut) periodic addition of small amounts of nutrients (1:1000 diluted ASW every 3-4 days) in the presence or absence of *R. pomeroyi* DSS-3. The arrow indicates the time point at which the addition of nutrients was stopped or *R. pomeroyi* was added. (f) Growth curves of axenic *Synechococcus* sp. WH7803 cultures in SW with periodic addition of small amounts of nutrients as shown in panel E, but ASW added was N, P or trace metals deplete. No nutrients were added in ‘Control’ cultures. The average value of triplicate cultures ( $n=3$ ) is shown in panels C-F (error bars show standard deviation).

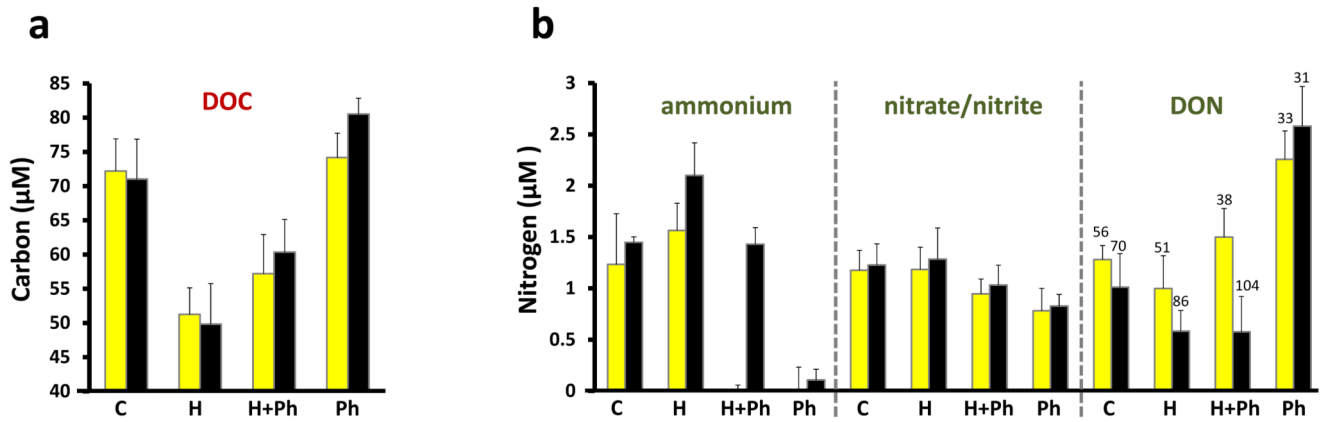


**Figure 4.**

Carbon (a) and nitrogen (b) nutrient analysis of SW (C), SW containing the heterotroph *R. pomeroyi* DSS-3 (H), SW containing the phototroph *Synechococcus* sp. WH7803 (Ph) and SW containing both microorganisms (H+Ph). DOC, ammonium, nitrate/nitrite and TN measurements were performed after seven days under optimum light conditions (yellow bars) and on the same cultures after a further seven days in the dark (black bars). DON was calculated after subtracting the inorganic N from TN. C:N ratios in each condition are indicated above the DON bars. The average value of triplicate cultures (n=3) is shown (error bars show standard deviation).

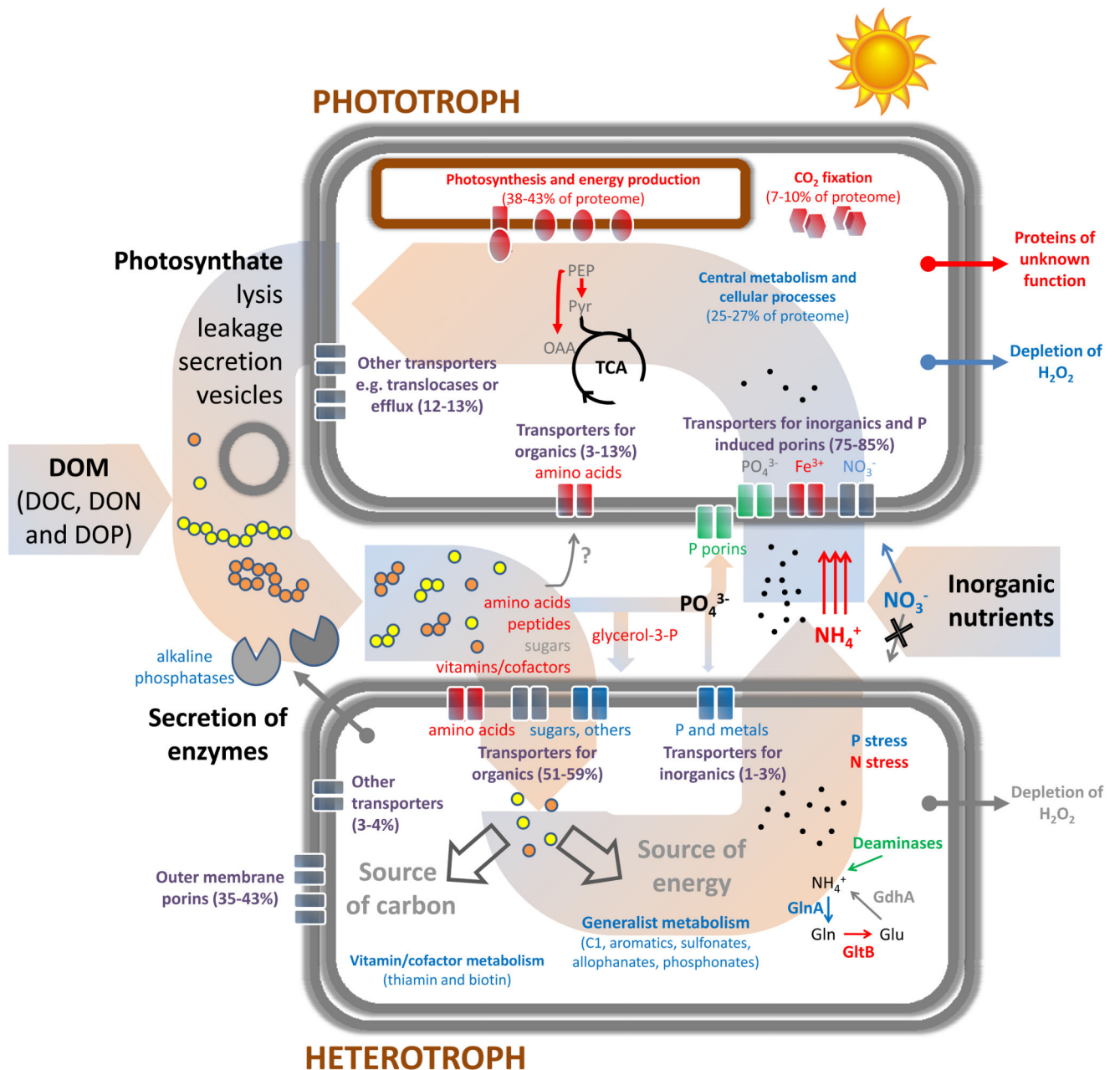


**Figure 5.** Schematic representation of the nutrient circulation process taking place in marine phototroph (*Synechococcus* sp. WH7803)-heterotroph (*R. pomeroyi* DSS-3) co-cultures in both ASW and SW conditions. Abundantly detected processes/pathways/transporters either higher (red) or lower (blue) in co-culture are represented in the phototrophic cell. Proteins with higher abundance in natural SW conditions are represented in green. The relative abundance of different groups of membrane transporters is also shown, summing 100% for each cell type. The abundance of other processes is relative to the total cellular proteome. PEP, phosphoenolpyruvate; Pyr, pyruvate; OAA, oxaloacetate; DOP, dissolved organic

phosphorous; TCA, tricarboxylic acid cycle; Gln, glutamine; Glu, glutamate; GlnA, glutamine synthase; GltB, glutamate synthase; GdhA, glutamate dehydrogenase.

**Table 1**

The abundance of *Synechococcus* sp. WH7803 protein categories detected in nutrient-rich ASW medium and natural seawater (SW)

	ASW (%)	SW (%)
Photosynthesis	37.7	34.0
Carbon fixation	7.0	9.5
Energy production and conversion	5.8	3.9
Basic cellular processes	16.4	16.2
Central metabolism	8.3	10.4
Inorganic nutrient processing	2.6	3.6
Membrane transport	2.4	9.3
Oxidative stress	4.3	2.5
Other cellular processes	2.6	1.9
Undefined	12.9	8.7



**Table 2**

*Synechococcus* sp. WH7803 proteins increased in abundance during co-culture with *R. pomeroyi* DSS-3 in nutrient-rich ASW medium compared to an axenic grown control culture (>2-fold increase and p-value < 0.01).

NCBI reference	Annotated function	Fold change	p-value
Unknown function			
YP_001224740.1	hypothetical protein SynWH7803_1017	38.7	<0.001
YP_001225429.1	hypothetical protein SynWH7803_1706	6.3	<0.001
YP_001225426.1	hypothetical protein SynWH7803_1703	5.5	0.010
YP_001226079.1	hypothetical protein SynWH7803_2356	4.7	0.003
YP_001226035.1	hypothetical protein SynWH7803_2312	3.0	0.009
Citric acid cycle			
YP_001224941.1	pyruvate kinase	5.5	0.007
YP_001224177.1	phosphoenolpyruvate carboxylase	2.4	0.001
Other functions			
YP_001224671.1	putative multicopper oxidase	5.4	<0.001
YP_001225564.1	twitching motility protein	5.1	<0.001
YP_001225795.1	ABC-type amino acid transport system	3.6	<0.001
YP_001224435.1	flavoprotein related to choline dehydrogenase	3.1	0.007
YP_001224753.1	N-acetylglucosamine-1-P uridyltransferase	2.6	0.002
YP_001224095.1	ribonucleases G and E	2.6	0.007
YP_001225323.1	protoporphyrin IX Mg-chelatase subunit ChII	2.1	0.005
Sugar metabolism and cell envelope			
YP_001224303.1	long-chain acyl-CoA synthetase	-7.9	<0.001
YP_001225887.1	phosphoglucomutase	-6.4	0.001
YP_001223965.1	UDP-glucose 4-epimerase	-2.0	0.003
Translation and protein processing			
YP_001224133.1	50S ribosomal protein L17	-4.3	0.001
YP_001224092.1	ATP-dependent Clp protease adaptor protein	-3.7	0.004
YP_001224152.1	50S ribosomal protein L22	-3.0	0.009
YP_001224147.1	50S ribosomal protein L14	-2.8	<0.001
YP_001224142.1	50S ribosomal protein L18	-2.8	<0.001
Nucleic acid biosynthesis, replication and transcription			
YP_001225172.1	two-component system response regulator	-3.9	0.004
YP_001224856.1	Uracil phosphoribosyltransferase	-3.0	<0.001
YP_001223749.1	hypothetical protein SynWH7803_0026	-2.5	0.006
YP_001224362.1	uridylylate kinase	-2.4	0.008
Biosynthesis of cofactors and secondary metabolites			
YP_001225094.1	pyridoxal phosphate biosynthetic protein PdxJ	-3.8	0.001
YP_001223792.1	hypothetical protein SynWH7803_0069	-2.1	0.004

NCBI reference	Annotated function	Fold change	p-value
YP_001224106.1	hypothetical protein SynWH7803_0383	-2.0	0.007
Amino acid biosynthesis			
YP_001223992.1	imidazoleglycerol-phosphate dehydratase	-3.7	0.003
YP_001225162.1	dihydrodipicolinate reductase	-2.3	<0.001
Electron transport			
YP_001226037.1	NAD(P)H-quinone oxidoreductase subunit H	-3.0	<0.001
YP_001225969.1	photosystem I assembly protein Ycf3	-2.1	0.008
Other functions			
YP_001226044.1	glutathione synthetase	-3.7	0.005
YP_001223895.1	rod shape-determining protein MreB	-2.7	0.007
YP_001223979.1	ABC-type transport system, ATPase comp.	-2.4	0.007
Unknown function			
YP_001225809.1	hypothetical protein SynWH7803_2086	-7.4	0.001
YP_001224473.1	hypothetical protein SynWH7803_0750	-3.8	0.001
YP_001225333.1	dienelactone hydrolase/uncharac. domain	-3.3	0.007
YP_001224023.1	hypothetical protein SynWH7803_0300	-2.2	0.003
YP_001225620.1	hypothetical protein SynWH7803_1897	-2.2	0.001
YP_001224075.1	hypothetical protein SynWH7803_0352	-2.1	0.008
YP_001224526.1	hypothetical protein SynWH7803_0803	-2.1	0.003
YP_001225623.1	hypothetical protein SynWH7803_1900	-2.1	0.001
YP_001225824.1	hypothetical protein SynWH7803_2101	-2.0	0.005